

Comfort Characterization of Various Fabrics for Extremity Protection

**by Wai Chin, Susan Gassett, Kyle Slusarski, Nancy Hibbert, Larry Long,
Mike Dalzell, and Eric D. Wetzel**

ARL-TR-6613

September 2013

NOTICES

Disclaimers

The findings in this report are not to be construed as an official Department of the Army position unless so designated by other authorized documents.

Citation of manufacturer's or trade names does not constitute an official endorsement or approval of the use thereof.

Destroy this report when it is no longer needed. Do not return it to the originator.

Army Research Laboratory

Aberdeen Proving Ground, MD 21005-5066

ARL-TR-6613**September 2013**

Comfort Characterization of Various Fabrics for Extremity Protection

Wai Chin, Kyle Slusarski, Larry Long, and Eric D. Wetzel
Weapons and Materials Research Directorate, ARL

Susan Gassett and Nancy Hibbert
Natick Soldier Research, Development, and Engineering Center

Mike Dalzell
Physical Protection Group, Defence Science and Technology Laboratory (UK)

REPORT DOCUMENTATION PAGE				Form Approved OMB No. 0704-0188	
Public reporting burden for this collection of information is estimated to average 1 hour per response, including the time for reviewing instructions, searching existing data sources, gathering and maintaining the data needed, and completing and reviewing the collection information. Send comments regarding this burden estimate or any other aspect of this collection of information, including suggestions for reducing the burden, to Department of Defense, Washington Headquarters Services, Directorate for Information Operations and Reports (0704-0188), 1215 Jefferson Davis Highway, Suite 1204, Arlington, VA 22202-4302. Respondents should be aware that notwithstanding any other provision of law, no person shall be subject to any penalty for failing to comply with a collection of information if it does not display a currently valid OMB control number. PLEASE DO NOT RETURN YOUR FORM TO THE ABOVE ADDRESS.					
1. REPORT DATE (DD-MM-YYYY) September 2013		2. REPORT TYPE Final		3. DATES COVERED (From - To) 18 June 2012–18 June 2013	
4. TITLE AND SUBTITLE Comfort Characterization of Various Fabrics for Extremity Protection				5a. CONTRACT NUMBER	
				5b. GRANT NUMBER	
				5c. PROGRAM ELEMENT NUMBER	
6. AUTHOR(S) Wai Chin, Susan Gassett,* Kyle Slusarski, Nancy Hibbert,* Larry Long, Mike Dalzell,† and Eric D. Wetzel				5d. PROJECT NUMBER	
				5e. TASK NUMBER	
				5f. WORK UNIT NUMBER	
7. PERFORMING ORGANIZATION NAME(S) AND ADDRESS(ES) U.S. Army Research Laboratory ATTN: RDRL-WMM-A Aberdeen Proving Ground, MD 21005-5066				8. PERFORMING ORGANIZATION REPORT NUMBER ARL-TR-6613	
9. SPONSORING/MONITORING AGENCY NAME(S) AND ADDRESS(ES)				10. SPONSOR/MONITOR'S ACRONYM(S)	
				11. SPONSOR/MONITOR'S REPORT NUMBER(S)	
12. DISTRIBUTION/AVAILABILITY STATEMENT Approved for public release; distribution is unlimited.					
13. SUPPLEMENTARY NOTES *Natick Soldier Research, Development, and Engineering Center, Textile Materials Evaluation Team, Natick, MA 01760 †Physical Protection Group, Defence Science and Technology Laboratory, Porton Down, UK Ministry of Defence, Wiltshire SP4 0JQ					
14. ABSTRACT Transport and mechanical properties for a range of knit, woven, and felted fabrics under consideration for extremity protection are reported. The textiles include: knits of silk, polyester, staple aramid, and continuous-filament aramid; plain woven nylon-cotton blend and continuous-filament aramid; and felted aramid and ultrahigh molecular weight polyethylene. Transport properties are characterized via water vapor transport at room temperature and body temperature (ASTM E 96), liquid moisture management (AATCC 195), air permeability (ASTM D 747), drying time, and horizontal wicking (AATCC 198). Mechanical properties are determined via uniaxial bending stiffness (ASTM D 1388), circular bending stiffness (ASTM 4032), stretch testing, and a novel test simulating knee-bend. The results show that the knits are likely to be most comfortable, as they offer high air and water vapor permeability with stretchability and low resistance to bending. Correlations between these measurements and garment comfort, as well as potential approaches for balancing comfort and protection requirements, are discussed.					
15. SUBJECT TERMS textile, fabric, armor, comfort, permeability, drape, stretch					
16. SECURITY CLASSIFICATION OF:			17. LIMITATION OF ABSTRACT UU	18. NUMBER OF PAGES 48	19a. NAME OF RESPONSIBLE PERSON Eric D. Wetzel
a. REPORT Unclassified	b. ABSTRACT Unclassified	c. THIS PAGE Unclassified			19b. TELEPHONE NUMBER (Include area code) 410-306-0851

Contents

List of Figures	v
List of Tables	vi
Acknowledgments	vii
1. Introduction	1
2. Experimental	2
2.1 Materials	2
2.2 Characterization of Transport Properties	6
2.2.1 Water Vapor Transmission at Room Temperature (Modified ASTM E 96)	6
2.2.2 Water Vapor Transmission at Body Temperature (Modified ASTM E 96).....	6
2.2.3 Liquid Moisture Management (AATCC 195).....	7
2.2.4 Air Permeability (ASTM D 737-04)	8
2.2.5 Drying Time (NSRDEC Method)	8
2.2.6 Horizontal Wicking (AATCC Test Method 198-2011)	9
2.3 Characterization of Mechanical Properties	9
2.3.1 Uniaxial Bending Stiffness (ASTM D 1388-08).....	9
2.3.2 Circular Bending Stiffness (ASTM 4032-08)	10
2.3.3 Stretchability	10
2.3.4 Knee-Bend Test	11
3. Results	13
3.1 Transport Properties	13
3.1.1 Water Vapor Transmission at Room Temperature.....	13
3.1.2 Water Vapor Transmission at Body Temperature.....	15
3.1.3 Liquid Moisture Management	16
3.1.4 Air Permeability	17
3.1.5 Drying Time	18
3.1.6 Horizontal Wicking	19
3.2 Mechanical Properties	20
3.2.1 Uniaxial Bending Stiffness.....	20
3.2.2 Circular Bending Stiffness	22

3.2.3 Stretchability	25
3.2.4 Knee-Bend Test.....	26
4. Discussion	28
4.1 Transport Properties	28
4.2 Mechanical Properties	28
4.3 Implications for Comfort.....	32
4.4 Correlating Comfort With Ballistic Performance	32
5. Conclusions	34
6. References	35
Distribution List	37

List of Figures

Figure 1. Photographs of fabrics before testing. Scales indicated in lower-right corners. (a) ACU, (b) K706, (c) silk, (d) light KK, (e) heavy KK, (f) polyester, (g) CFKA, (h) hydroentangled Dyneema (HED), (i) ArmorFelt, and (j) TexTech.	4
Figure 2. (a) Sample cup with water and (b) with fabric clamped and sealed.	7
Figure 3. Moisture management tester Model M290 from SDL-Atlas.	7
Figure 4. Air permeability tester, TexTest model FX 3300 from Advanced Testing Instruments.	8
Figure 5. Horizontal wicking test setup.	9
Figure 6. Fabric bending stiffness was measured with a Shirley Stiffness Tester model M003B from SDL-Atlas.	9
Figure 7. Circular bend test apparatus (orifice not visible).	10
Figure 8. Photograph of the stretch test.	11
Figure 9. Knee-bend test apparatus: (a) full operation and (b) central linkage only.	12
Figure 10. Average water vapor transport of materials in 24 h; error bars indicate standard deviation of each averaged value.	13
Figure 11. Average water vapor transport in g/hr·m ² for different fabrics in 73 °F, 50 ± 2% RH; derived from 24-h results divided by 24.	14
Figure 12. Average water mass loss as a function of time for two layers of fabrics.	15
Figure 13. Average water vapor transmission of materials at 37 °C, 15% ± 2% RH.	16
Figure 14. Overall moisture management capabilities rating of one-layer fabrics.	17
Figure 15. Average air permeability in cubic centimeters per second per square centimeter; error bars indicate standard deviation of each averaged value.	18
Figure 16. Drying time in minutes for different fabrics.	19
Figure 17. Horizontal liquid transport in millimeters per 5 min.	20
Figure 18. Uniaxial stiffness test results—bending stiffness and flexural rigidity.	21
Figure 19. Load displacement data for circular bend test: (a) linear scale and (b) log scale.	23
Figure 20. Maximum loads generated during circular bend test.	24
Figure 21. Load extension data for stretch test.	25
Figure 22. Normalized load displacement data for knee-bend test.	27
Figure 23. Maximum normalized load data during knee-bend test.	27
Figure 24. Circular bend peak load as a function of fabric thickness.	29
Figure 25. Thickness-normalized maximum load data from circular bend test.	30
Figure 26. Density-normalized maximum load data from knee-bend test.	31
Figure 27. Ballistic metric (density-normalized V ₅₀) as a function of comfort metric (density-normalized knee-bend force).	33

List of Tables

Table 1. Evaluated fabrics. Areal density values are manufacturer values, except for polyester and continuous fiber knitted aramid (CFKA) fabrics, which were experimentally measured.	3
Table 2. Summary of fabric characterizations performed.	5
Table 3. Conversion table for MMC rating to fabric grading.....	8
Table 4. Average water vapor transport of materials in 24 h with standard deviation.	14
Table 5. Average water vapor transport in g/hr·m ² for different fabrics in 73 °F, 50 ± 2% RH; derived from 24-h results divided by 24.	15
Table 6. Water vapor transport for different fabrics.	16
Table 7. Overall MMC rating and moisture management grading for each fabric.....	17
Table 8. Average air permeability in cubic centimeter per second (cm ³ /s/cm ²).....	18
Table 9. Drying time in minutes for different fabrics.	19
Table 10. Horizontal liquid transport in millimeters per 5 min.	20
Table 11. Bending stiffness and flexural rigidity from uniaxial bending tests.....	21
Table 12. Maximum loads during circular bend test.	24
Table 13. Maximum loads during stretch test.....	26
Table 14. Maximum normalized loads during knee-bend test.....	31
Table 15. V ₅₀ and knee-bend test data normalization. Ballistic data from Michael et al.	33

Acknowledgments

The authors would like to thank Paul Nenno of the U.S. Army Research Laboratory (ARL) for assistance in formatting many of the plots and tables; Josh Taggart of ARL for assistance with thickness measurements; Luisa DeMoraes, Melynda Perry, and Amy Bicica of the U.S. Army Natick Soldier Research, Development, and Engineering Center for providing technical guidance, support, and moisture management data analysis summary.

INTENTIONALLY LEFT BLANK.

1. Background

The U.S. Army is currently engaged in a program to provide Soldiers with ballistic protective undergarments (PUGs) and protective over garments (POGs) to reduce the number of injuries caused by buried improvised explosive devices. It is important for the chosen fabric materials to not only resist sand, dirt, and other debris at high velocities but also conform to the body and wear comfortably over a long period of time. The U.S. Army is also more generally interested in the development of lightweight extremity protection to provide enhanced protection to arms, legs, and neck against shrapnel and accelerated debris.

Typically, the performance of armor systems is evaluated by comparing their ballistic performance (typified by V_{50}) against areal density. However, areal density may not be a sufficient metric for extremity and PUG/POG applications. The protection levels and, therefore, ply counts and areal densities of these armors are likely to be much lower than conventional armors (such as the standard outer tactical vest [OTV]). Therefore, these armors will inherently be very light, and therefore further reductions in mass are unlikely to be perceived by the wearer. In addition, these garments will likely be worn over body joints such as hips, knees, and elbows, where high stretch and flexibility may be critical for maintaining desired freedom of motion. Finally, because such garments could be in near-skin contact and could potentially be used to drastically increase the amount of armor coverage on a wearer, the thermal and moisture transport properties of these fabrics are highly relevant to Soldier comfort.

The physical burden or comfort of a garment is likely to be influenced by the design and tailoring of the garment and the physical properties of the material from which it is made. Of these two factors, design and tailoring are somewhat more subjective and difficult to quantify, whereas physical properties are generally easier to characterize.

The physical characteristics of a fabric that might affect burden and comfort can be categorized as follows (*1*):

Mass/volume properties

- Areal density
- Thickness

Transport properties

- Thermal resistance
- Air permeability
- Moisture vapor permeability

- Through-thickness and horizontal moisture management (wicking)
- Drying time

Mechanical properties

- In-plane extensional modulus and maximum elastic strain
- Bending stiffness
- In-plane shear stiffness
- Surface roughness and friction, relative to skin/hair and other fabrics

In addition, it is recognized that burden and comfort may also be a function of less well-characterized properties such as fabric “drape” (i.e., the ability to conform to a surface), which is thought to be a function of bending and in-plane shear stiffness (2). Some tests physically combine elements from the previous list, such as the guarded sweating hotplate test, which measures elements of both thermal resistance and permeability (3).

Other tests have been developed to quantify the overall comfort of body armor garments. One approach is to execute “wear trials,” where a series of human subjects are asked to wear body armor, execute planned motions, and then quantify performance based on qualitative comfort metrics (4). A limitation of wear trial methods is that they require considerable effort to staff and execute, do not provide consistent engineering data, and do not generate any fundamental insights into the material, mechanical, and design features that drive perceived comfort. Horsfall et al. (4) attempted to create a laboratory test for predicting comfort in torso body armor systems based on a hemispherical bend test. The results showed good overall correlation with wear trials. However, this specific approach is not directly applicable to the study of ballistic undergarments, where garments are much thinner, require much more flexibility, and require management of thermal and moisture properties.

The objective of this study is to characterize candidate extremity, PUG, and POG materials relative to properties that determine overall system comfort. This data, when combined with ballistic data (5), provides a more complete assessment of the relative performance of various materials for extremity and PUG/POG applications.

2. Experimental

2.1 Materials

Tested fabrics are summarized in table 1, with references to macroscopic photographs in figure 1. Each photograph shows untested material.

Table 1. Evaluated fabrics. Areal density values are manufacturer values, except for polyester and continuous fiber knitted aramid (CFKA) fabrics, which were experimentally measured.

Sample name	Description	Part number	Source	Areal density (g/m ²)	Thickness (mm)
ACU	"Improved Defender M" Fire Resistant ACU fabric	-	Tencate (Almelo, Netherlands)	220	0.36
K706	woven 600d KM2 Kevlar	Style 706	JPS Composites (Anderson, SC)	180	0.25
Silk	knitted Jersey silk	-	NY Fashion Center (New York City, NY)	165	0.31
Light KK	"light" knitted staple Kevlar	145KV37	Green Mountain Knitting (Milton, VT)	225	1.23
Heavy KK	"heavy" knitted staple Kevlar	437KV17	Green Mountain Knitting (Milton, VT)	328	1.63
Polyester	knitted polyester	-	Jo-Ann Fabrics (Bel Air, MD)	96	0.52
CFKA	continuous fiber knitted KM2 600d Kevlar	-	NSRDEC (Natick, MA)	200	0.63
HED	hydroentangled Dyneema felt	-	UK Ministry of Defense	200	0.83
ArmorFelt	Armorfelt, hybrid aramid/PE felt	-	Kennon Covers Inc. (Sheridan, WY)	250	2.71
TexTech	hybrid felt / woven fabric	9010	TexTech Industries (Portland, ME)	844	1.93

Note: ACU = Army Combat Uniform.

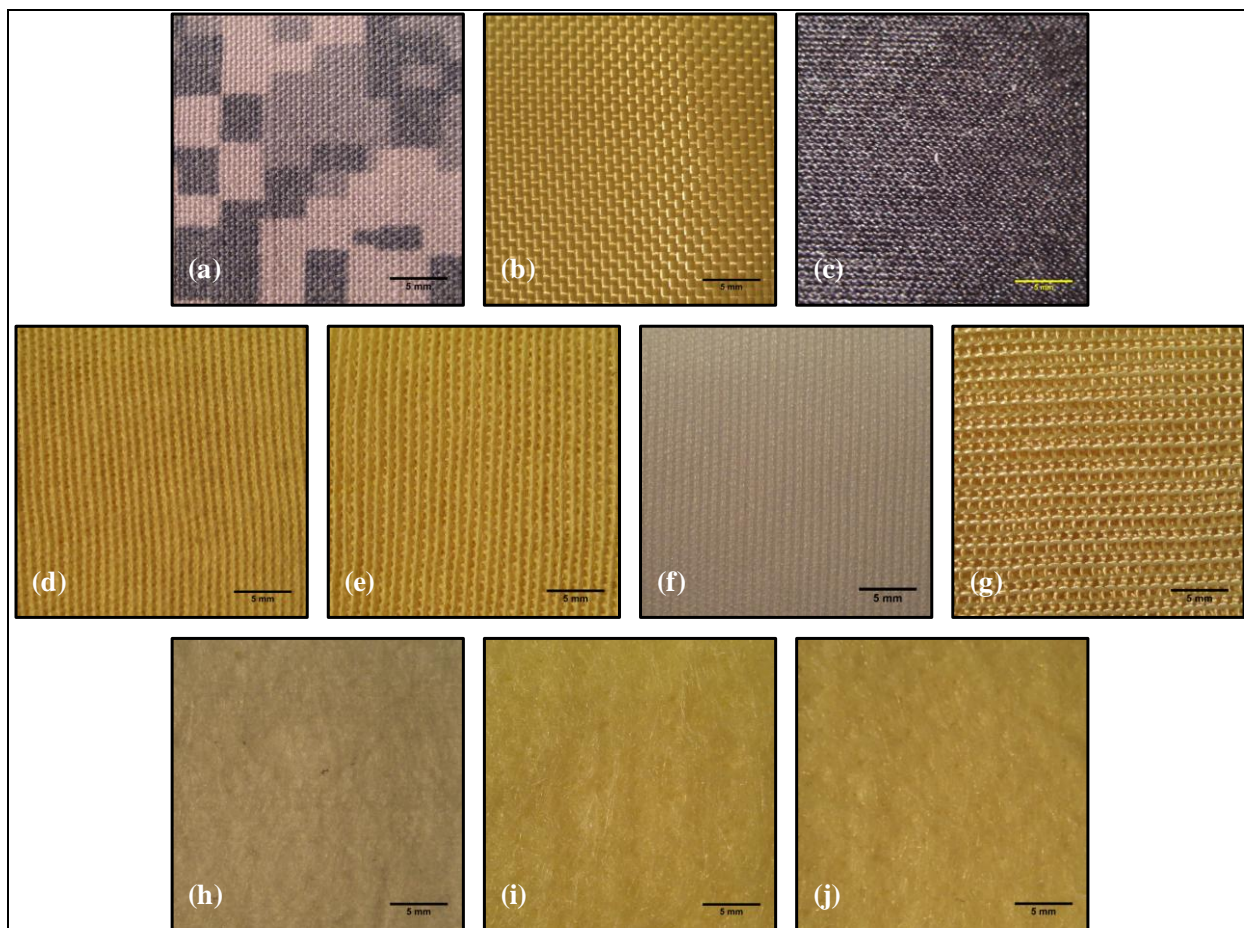


Figure 1. Photographs of fabrics before testing. Scales indicated in lower-right corners. (a) ACU, (b) K706, (c) silk, (d) light KK, (e) heavy KK, (f) polyester, (g) CFKA, (h) hydroentangled Dyneema (HED), (i) ArmorFelt, and (j) TexTech.

The ACU fabric represents the nominal Army Combat Uniform fabric currently worn. Woven Kevlar K706 fabric is representative of the fabrics used to provide ballistic protection in the current OTV.

The knitted silk fabric is very similar to silk fabrics used in ballistic undergarments recently fielded by U.S. and United Kingdom (UK) militaries (6, 7). The light and heavy knitted Kevlars are representative of commodity knitted Kevlars used in sporting goods and cut-resistant gloves. Note that these knitted Kevlars are produced using discontinuous, stretch-broken staple yarns. The polyester fabric represents a typical lightweight, stretchable, synthetic commercial comfort fabric.

The CFKA is knit from unbroken, continuous fiber 600d KM2 yarns identical to those used in the woven KM2 fabric. The CFKA knits were made at the U.S. Army Natick Soldier Research, Development, and Engineering Center (NSRDEC) in Natick, MA. These samples were produced in approximately 7-cm-diameter socks that were sliced into larger, approximately 20-cm-wide strips that were stacked to create multilayer samples.

Hydro-entangled felts made from ultra-high-molecular-weight polyethylene (UHMWPE) were provided by the Defence Science and Technology Laboratory, U.K. Ministry of Defence. ArmorFelt is a commercial product composed of felted aramid and UHMWPE fibers. TexTech is a hybrid multilayer fabric composed of a felted aramid and a woven aramid that are needle-punched together with staple aramid fibers. This fabric has a considerably higher areal density compared to the other fabrics evaluated.

Areal density values in table 1 are manufacturer values, except for the polyester and CFKA fabrics, which were experimentally measured. For these samples, fabric swatches that ranged in size from approximately 15.2×15.2 cm to 305×305 cm were cut and weighed, with the areal density calculated as mass normalized by area. Because knits are stretchable, the areas used for areal density calculations were based on the area at a degree of stretch representative of the as-tested state of the material. This state is typically achieved with a slight tension, enough to remove wrinkles but not sufficient to significantly distort the knit architecture.

Thickness values in table 1 were measured using a modified version of ASTM D 1777-96 (8). A flat platen was mounted to the fixed base of an MTS Synergie load frame with a 500-N load cell. A cylindrical presser foot with a diameter of 26 mm (ASTM D 1777 calls for a 28.7-mm-diameter presser foot) was mounted to the crosshead so that the circular flat face of the foot was parallel to the lower platen. The crosshead was moved downward until it engaged the lower platen. At this point the crosshead displacement was set to zero. The crosshead was then raised, the fabric was placed on the platen, and then the crosshead was lowered into the fabric at a rate of 1.27 mm/min. The height of the crosshead above the lower platen, at a load of 4.14 kPa (0.60 psi, corresponding to a load of 2.20 N), is reported as the fabric thickness. Three samples were tested for each fabric, and the average thickness is reported to the nearest 0.01 mm.

Table 2 lists the experiments performed for each material type.

Table 2. Summary of fabric characterizations performed.

Sample name	Transport properties						Mechanical properties			
	Water vapor transport, room temperature	Water vapor transport, body temperature	Liquid moisture management	Air permeability	Drying time	Horizontal wicking	Uniaxial bending stiffness	Circular bending stiffness	Stretchability	Knee bend test
ACU	X	X	X	X	X	X	X	X	X	X
K706		X						X	X	X
Silk	X	X	X	X	X	X	X	X	X	X
Light KK	X	X	X	X	X	X	X	X	X	X
Heavy KK	X	X	X	X	X	X	X	X	X	X
Polyester		X						X	X	X
CFKA		X						X	X	X
HED	X	X	X	X	X	X	X	X	X	X
ArmorFelt								X	X	X
TexTech									X	X

2.2 Characterization of Transport Properties

2.2.1 Water Vapor Transmission at Room Temperature (Modified ASTM E 96)

Breathability measurements were performed based on ASTM E 96/E 96M-10 (9).

Approximately 100 g of distilled water was placed in a 150-mL (76.2-mm-diameter × 50.8-mm-high) diffusion cup at room temperature. The mass of the water was carefully weighed and recorded. A 76.2-mm-diameter circle of fabric was then placed on top of the diffusion cup with a 63.5-mm-diameter circular exposed surface and sealed using a threaded lid. The mating faces of the lid and container have interlocking grooves to seal the fabric edges, so no secondary sealant material, such as wax, was required. The cup, water, and fabric were weighed and then placed in a small bench-top humidity chamber specifically designed for textile evaluation. Temperature and humidity were monitored and controlled internally by built-in calibrated instrumentation, with testing taking place over a period of 24 h at 22.8 ± 0.6 °C (73 ± 1 °F), and $50\% \pm 2\%$ RH. For RT measurements, a single layer of fabric was evaluated.

Weight-loss measurements were performed by removing the diffusion cup from the humidity chamber and weighing and recording total system mass. Measurements were taken initially and after a 24-h exposure period. Three samples of each material type were characterized with average values reported.

2.2.2 Water Vapor Transmission at Body Temperature (Modified ASTM E 96)

Additional water vapor transmission experiments were performed at body temperature to simulate near-skin textile performance while worn, and at dry conditions to simulate an arid environment. The test method was similar to the RT method but with a testing period of 72 h at 37 °C and $15\% \pm 2\%$ RH. Approximately 30 g of distilled water was placed in a 50-mL (50.8-mm-diameter × 25.4-mm-high) diffusion cup at RT (figure 2a). The mass of the water was carefully weighed and recorded. A 67-mm-diameter circle of fabric was then placed on top of the diffusion cup with a 50-mm-diameter circular exposed surface and sealed using a threaded lid (figure 2b). Testing was performed in a Caron 6030 humidity chamber, and a stack of two layers of fabric were evaluated. Weight-loss measurements were taken at 4-h intervals on the first day, with a longer break while samples continued overnight, and then three times per day for a total of 72 h or until sufficient data were gathered to determine the constant weight-loss rate of the samples.

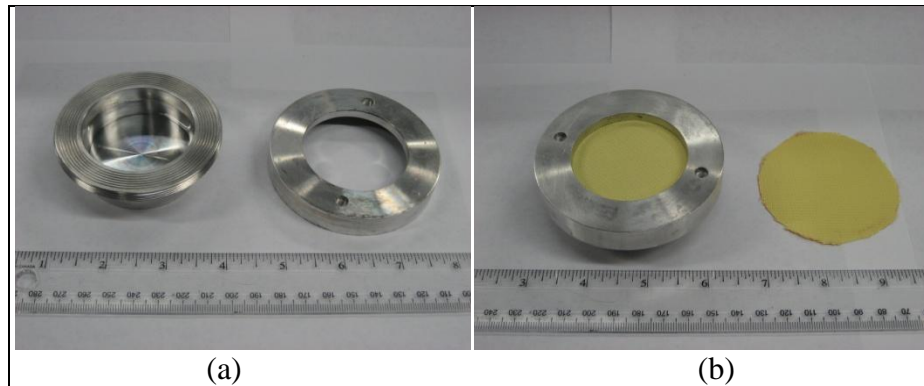


Figure 2. (a) Sample cup with water and (b) with fabric clamped and sealed.

2.2.3 Liquid Moisture Management (AATCC 195)

The liquid moisture management properties of textiles were measured using a Model M290 moisture management tester from SDL-Atlas (Rock Hill, SC), shown in figure 3. This test method, American Association of Textile Chemists and Colorists (AATCC) 195, is intended to provide information on how fabrics would respond to human perspiration. Measurements are performed by placing a fabric specimen between two electrode arrays that measure electrical resistance over various electrode pairings across the specimen (10). The resulting readings are used to calculate fabric moisture changes that quantify multiple modes of water transport in the fabric. The results of this test method yield the following parameters:

- Wetting time, top and bottom layers, in seconds
- Absorption rate, top and bottom, in percent per second
- Maximum wetted radius, top and bottom, in millimeters
- Spreading speed in millimeters per second
- One-way transport capability index, in percent
- Overall moisture management capability (MMC) rating, a combined metric for fabric liquid moisture transport. The MMC rating is used to assign a grading to the fabric from 1 to 5 with 1 = poor, 2 = fair, 3 = good, 4 = very good, and 5 = excellent (table 3).



Figure 3. Moisture management tester Model M290 from SDL-Atlas.

Table 3. Conversion table for MMC rating to fabric grading.

MMC Rating	Grading
0.00 - 0.19	Poor
0.20 - 0.39	Fair
0.40 - 0.59	Good
0.60 - 0.80	Very Good
>0.80	Excellent

2.2.4 Air Permeability (ASTM D 737-04)

Air permeability is measured according to ASTM D 737-04 (11), using a TexTest model FX3300 from Advanced Testing Instruments (Greer, SC) (figure 4). The rate of air flow passing perpendicularly through a known area of fabric is adjusted to obtain a prescribed air pressure differential between the two fabric surfaces. From this rate of air flow, the air permeability of the fabric is determined.



Figure 4. Air permeability tester, TexTest model FX 3300 from Advanced Testing Instruments.

2.2.5 Drying Time (NSRDEC Method)

In this test method, a pretreated wet specimen is sandwiched between two pieces of unused blotting paper, passed through a wringer with a dead weight load of 27.7 ± 0.5 kg, and dried to constant weight in the standard condition of $65 \pm 2\%$ RH and 70 ± 2 °F (12). Drying time was measured with the Adams Model AAA 250L electronic digital analytical balancer and EK-i/EW-I-series Labtronics, Inc., software.

2.2.6 Horizontal Wicking (AATCC Test Method 198-2011)

The AATCC horizontal wicking test method 198-2011 (13) measures the transport rate of liquid along and through the horizontally aligned fabric specimens (figure 5). A volume of water is deposited with a burette mounted above a fabric sample, which is mounted to a beaker using an embroidery hoop. The rate of horizontal wicking is visually observed and manually timed, measured, and recorded.

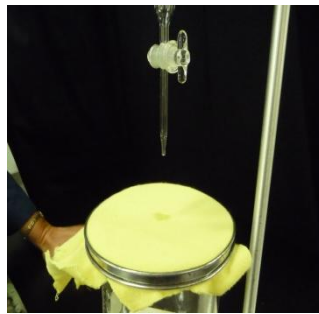


Figure 5. Horizontal wicking test setup.

2.3 Characterization of Mechanical Properties

2.3.1 Uniaxial Bending Stiffness (ASTM D 1388-08)

Fabric stiffness was measured according to ASTM D 1388-08 (14), using a Shirley Stiffness Tester model M003B from SDL-Atlas (figure 6). The tester gradually slides the fabric sample along a base plate so that its free end extends as a cantilever with increasing length. When the sample bends under its own weight to an angle of at least 41.5° the cantilevered length is recorded. The flexural rigidity is calculated from this measured length.



Figure 6. Fabric bending stiffness was measured with a Shirley Stiffness Tester model M003B from SDL-Atlas.

2.3.2 Circular Bending Stiffness (ASTM 4032-08)

A limitation of ASTM D 1388 is that it evaluates only simple fabric bending along one axis. In contrast, garments undergo more complex multiaxial bending scenarios to accommodate wearer motion. To address multiaxial bending, ASTM 4032-08 (15) executes a circular bending action by forcing the fabric of interest through a circular orifice and determining the maximum force required to do so. A picture of the experimental setup appears in figure 7.

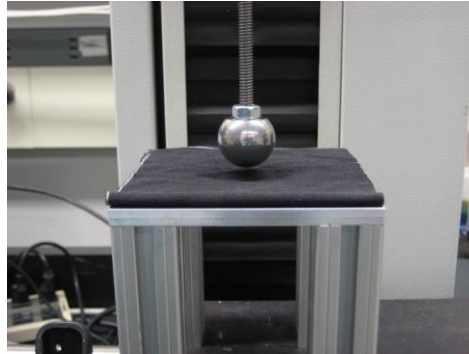


Figure 7. Circular bend test apparatus (orifice not visible).

To perform the circular bend test, 10.2- × 20.3-cm swatches of test fabrics were folded in half and allowed to rest on a steel platform containing a tapered orifice. In each case, the fabric was oriented so that the fold was aligned with the front edge of the platform. A 2.54-cm-diameter plunger was mounted into the 500-N load cell of an MTS Synergie load frame using a pin connection and then tightened with a screw collar to remove slack from the load path. The plunger was mounted concentrically with respect to the 3.81-cm-diameter orifice plate, with 0.635 cm of clearance on all sides, and then moved into a starting position 0.318 cm above the surface of the platform. In cases where fabric thicknesses could not accommodate this position, the plunger was moved into a starting position 0.635 cm above the plate. The load frame was programmed to give a plunger stroke length of 57 mm, a stroke rate of 1000 mm/min, and a data acquisition rate of 64 Hz.

2.3.3 Stretchability

The stretch test, shown in figure 8, is designed to measure the mechanical response of fabrics when pulled in the stretch direction. Fabrics with high resistance to stretch are generally stiffer and less comfortable than compliant fabrics. To prepare for the test, 25.4- × 7.62-cm rectangular strips of each fabric were cut from bulk. The fabric was oriented so that the long dimension of each swatch was parallel with the stretch direction. Both ends of each strip were folded over 2.54 cm and sewn to increase the thickness of the fabric in the gripping region, thus creating specimens with 15.2- × 7.62-cm rectangular gage areas.

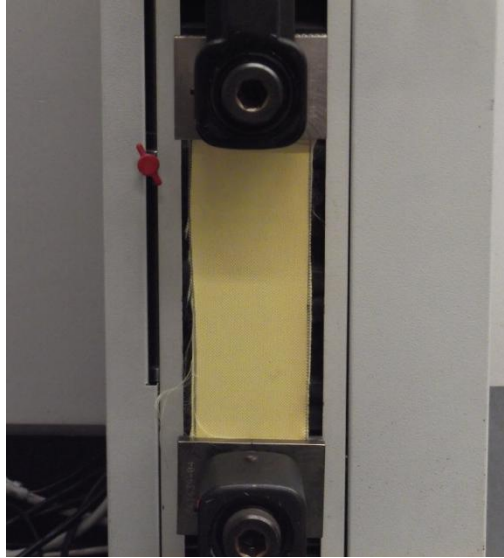


Figure 8. Photograph of the stretch test.

To perform the test, fabric specimens were loaded into a MTS Synergie load frame using mechanical screw grips. Specimens were orientated so the long dimension was parallel with the load path. A 500-N load cell was used to perform all tests. Fabrics were pulled at a rate of 16 mm/min through 8 mm of extension.

2.3.4 Knee-Bend Test

A limitation of the circular bend test is that the ball-orifice gap is fixed, resulting in insertion forces that are strongly influenced by fabric thickness. This design aspect could lead to artificially high stiffness data for thicker fabrics, such as felts. A better test would evaluate multiaxial fabric stiffness without gap effects.

Figure 9 shows a prototype knee-bend test under development at U.S. Army Research Laboratory. The fabric of interest is wrapped around a cylindrical foam substrate encasing a hinged aluminum linkage. The ends of the linkage are connected to a load frame using accessory grips and then loaded in compression. Rotation about the hinges forces the foam cylinder to bend, and the resistance to bending is measured and recorded. The relative change in bending resistance caused by the addition of fabric layers can then be quantified. Unlike the circular bend test, the knee-bend test is not gap-dependent. The fabric on the front of the knee is subject to positive-positive curvature bending (tension in both orthogonal axes), while the fabric on the back of the knee is subject to positive-negative curvature bending (a saddle point with tension along one axis and compression along the other axis).

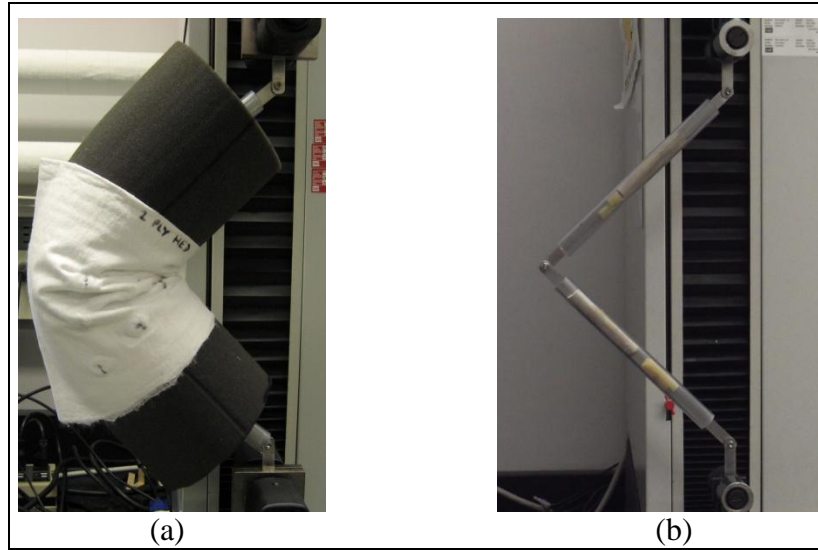


Figure 9. Knee-bend test apparatus: (a) full operation and (b) central linkage only.

For the present study, the foam wrapping for the knee-bend test is super-cushioning polyurethane foam, McMaster-Carr part number 8875K16, with a 15.2-cm diameter and a length of 45.7 cm, with a 0.476-mm-diameter cylindrical hole bored out of the center. The center linkage assembly is made of 1.59-mm-thick aluminum sheared into 1.27-cm-wide strips, two at 27.9 cm long and two at 10.2 cm long. The ends of these strips are rounded to remove any sharp edges, and the links are connected together using nonloosening nuts. Two pieces of 1.27-cm-inner-diameter polyvinyl chloride (PVC) tube were placed over the linkage prior to insertion to prevent cutting of the surrounding foam.

To perform the knee-bend test, the foam-linkage assembly was placed in an MTS Synergie load frame with a 500-N load cell. The crosshead was then positioned so that the two main links were oriented at 20° from the vertical axis to avoid excessive compressive loads and buckling effects during start-up. The load frame was programmed to give a stroke length of 200 mm, a stroke rate of 400 mm/min, and a data acquisition rate of 33 Hz. The stroke length of 200 mm corresponds with 35° of frame member rotation, which in turn corresponds to 70° of center hinge angle change.

Before fabric testing, the foam cylinder was conditioned by running several tests to break-in the material. This was done because the tendency of the foam to stiffen over time affected data consistency. A brief study was conducted to determine the minimum number of tests needed to yield reproducible loads in the foam and the optimum amount of time between tests to avoid foam stiffening. These values were found to be 10 tests and 60 s, respectively. For the purposes of this experiment, reproducibility was defined as the first instance of five consecutive load values each within ± 0.005 N of their average. After conditioning, two-ply swatches of fabric were wrapped around the foam cylinder. Ten tests were conducted for each fabric. To evaluate

the effect of each fabric on resistance to bending, the 10th test for each fabric was normalized by subtracting out the bending resistance contributed by the foam. The normalized load displacement curves were then plotted on the same graph to assess differences among materials.

3. Results

3.1 Transport Properties

3.1.1 Water Vapor Transmission at Room Temperature

Figures 10 and 11 and tables 4 and 5 show the average water moisture vapor transport at RT and 50% RH for single-layer samples. The high vapor transmission materials are the two knitted Kevlars, most likely due to their relatively open knitted structures. The lower vapor transmission materials are the ACU woven cloth and the HED felt. The tightly knitted silk cloth is slightly better in vapor transmission than the ACU, our baseline material.

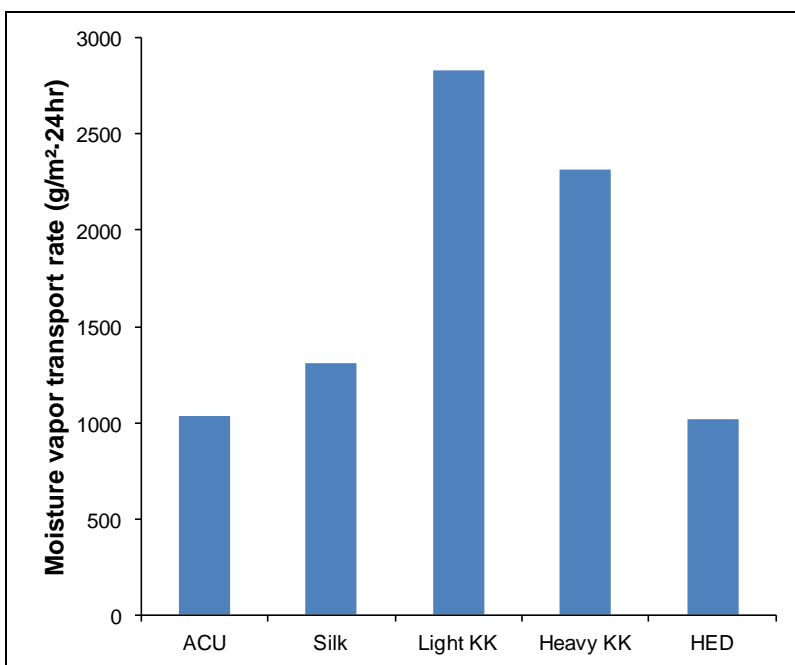


Figure 10. Average water vapor transport of materials in 24 h; error bars indicate standard deviation of each averaged value.

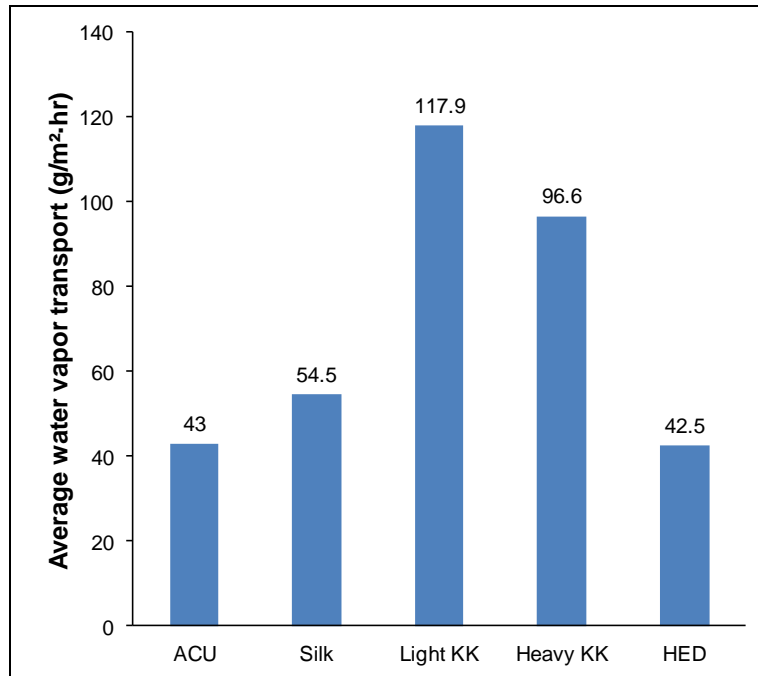


Figure 11. Average water vapor transport in g/h·m² for different fabrics in 73 °F, 50 ± 2% RH; derived from 24-h results divided by 24.

Table 4. Average water vapor transport of materials in 24 h with standard deviation.

Run number	Moisture vapor transport rate (g/m ² ·24hrs)				
	ACU	Silk	Light KK	Heavy KK	HED
1	1013	1303	2906	2418	1003
2	1041	1348	2715	2326	1005
3	1039	1274	2870	2210	1050
Ave	1031	1308	2830	2318	1019
Std dev	16	37	101	104	27

Table 5. Average water vapor transport in $\text{g/h}\cdot\text{m}^2$ for different fabrics in 73 °F, $50 \pm 2\%$ RH; derived from 24-h results divided by 24.

Sample ID	Water vapor transport ($\text{g/m}^2\cdot\text{hr}$)
ACU	43
Silk	54.5
Light KK	117.9
Heavy KK	96.6
HED	42.5

3.1.2 Water Vapor Transmission at Body Temperature

Figure 12 shows water mass loss as a function of time for each two-layer sample in this extended-duration test at body temperature and low humidity. Mass loss occurs at a relatively constant rate for each material. The slopes of these lines are used to estimate an average mass loss rate for each fabric, as given in figure 13 and table 6. The CFKA sample shows the highest vapor transmission, which is not surprising given its loosely knitted structure. The K706 material shows the lowest vapor transmission, likely due to its tightly woven structure. All of the knit materials (silk, light KK, heavy KK, polyester, and CFKA) exhibit good water vapor transmission.

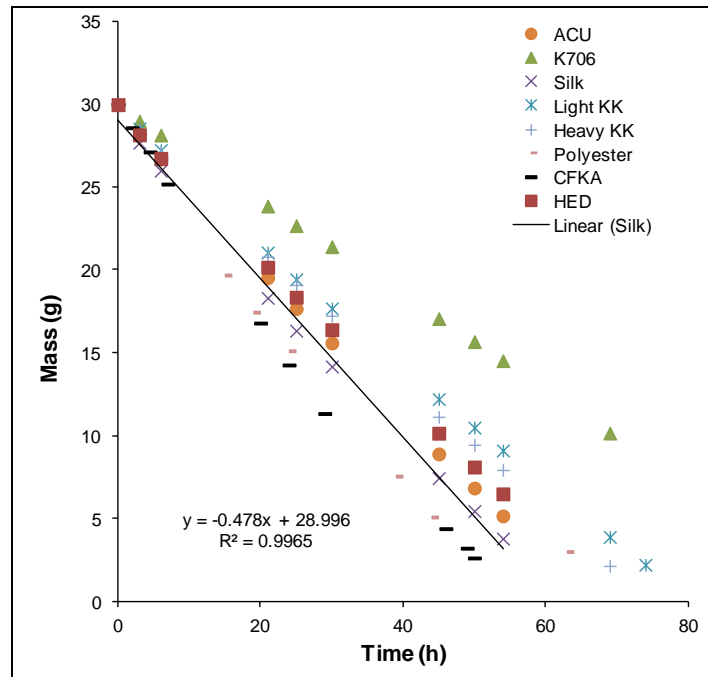


Figure 12. Average water mass loss as a function of time for two layers of fabrics.

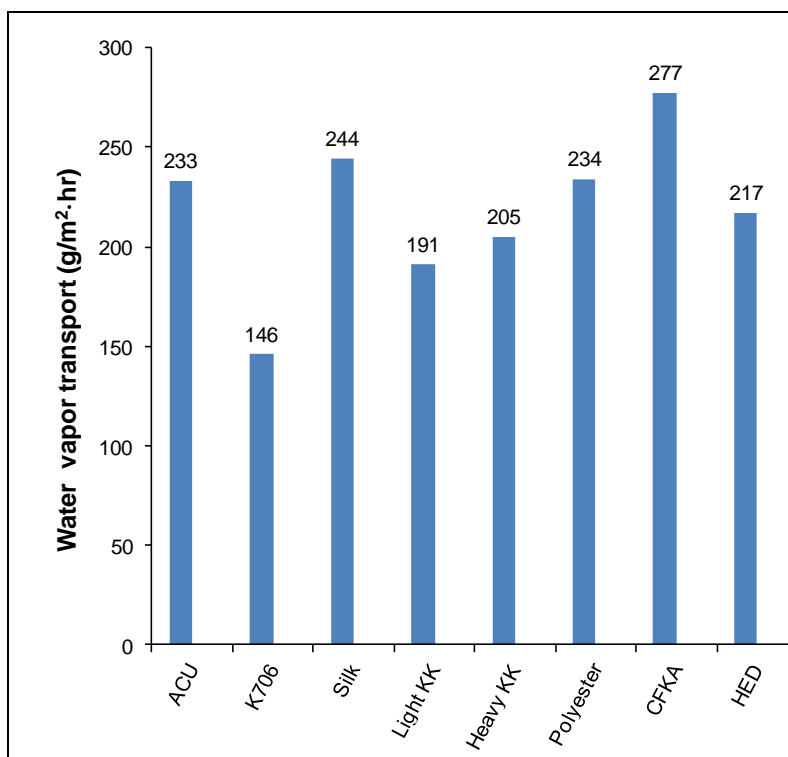


Figure 13. Average water vapor transmission of materials at 37 °C, 15% ± 2% RH.

Table 6. Water vapor transport for different fabrics.

Sample ID	Water vapor transport (g/m ² ·hr)
ACU	233
K706	146
Silk	244
Light KK	191
Heavy KK	205
Polyester	234
CFKK	277
HED	217

3.1.3 Liquid Moisture Management

Figure 14 and table 7 show MMC ratings for the fabrics evaluated. Silk, light KK, and ACU are given ratings of “Very Good,” while HED is given a “Poor” rating. These results suggest that HED fabric, when worn close to the skin, could present challenges for management of perspiration. Specifically, the HED fabric has very low “wettability,” so perspiration might be trapped at the skin rather than being transported away to enable perspiration-driven body cooling.

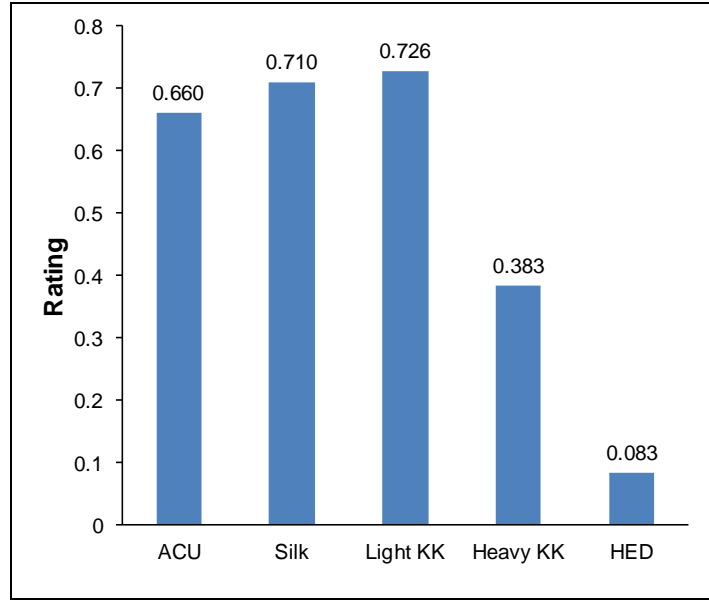


Figure 14. Overall moisture management capabilities rating of one-layer fabrics.

Table 7. Overall MMC rating and moisture management grading for each fabric.

Sample ID	MMC Rating	Grading
ACU	0.660	Very Good
Silk	0.710	Very Good
Light KK	0.726	Very Good
Heavy KK	0.383	Fair
HED	0.083	Poor

3.1.4 Air Permeability

Figure 15 and table 8 show results of air permeability. The data indicate that the knits (silk, light KK, and heavy KK) exhibit good air permeability, likely due to their open structure. In contrast, the ACU and HED fabrics offer relatively low permeability.

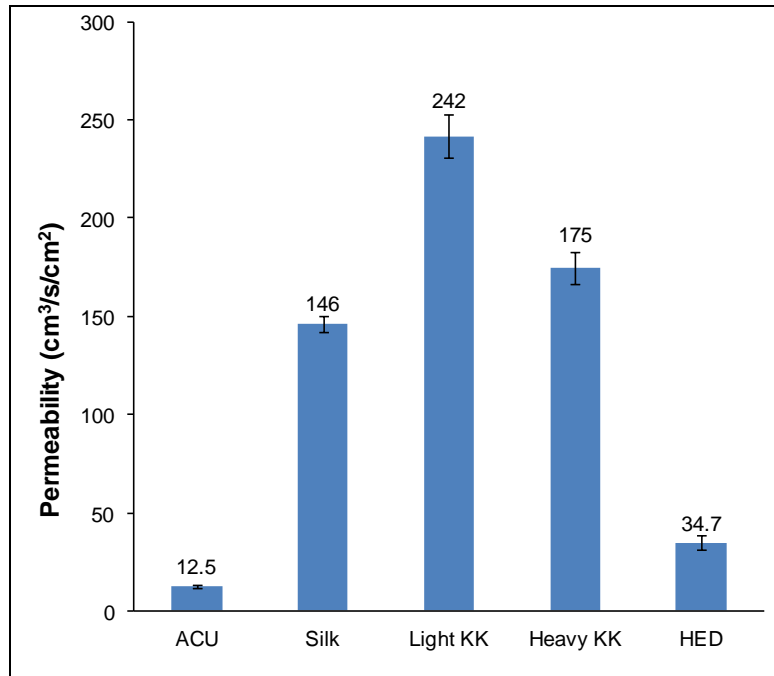


Figure 15. Average air permeability in cubic centimeters per second per square centimeter; error bars indicate standard deviation of each averaged value.

Table 8. Average air permeability in cubic centimeter per second ($\text{cm}^3/\text{s}/\text{cm}^2$).

Sample ID	Permeability ($\text{cm}^3/\text{s}/\text{cm}^2$)				
	Run 1	Run 2	Run 3	Ave.	Std. dev.
ACU	13.7	11.7	12.2	12.5	1.1
Silk	144	144	151	146	4.0
Light KK	239	232	254	242	11.1
Heavy KK	183	175	166	175	8.4
HED	35.1	38.1	31.0	34.7	3.6

3.1.5 Drying Time

Figure 16 and table 9 show the drying time results in minutes. The HED dries the fastest, and the ACU fabric also dries relatively quickly. The Kevlar knits exhibit the longest drying times. Faster drying times are expected to correlate with better comfort, as saturated garments (whether from perspiration or precipitation) are uncomfortable to wear.

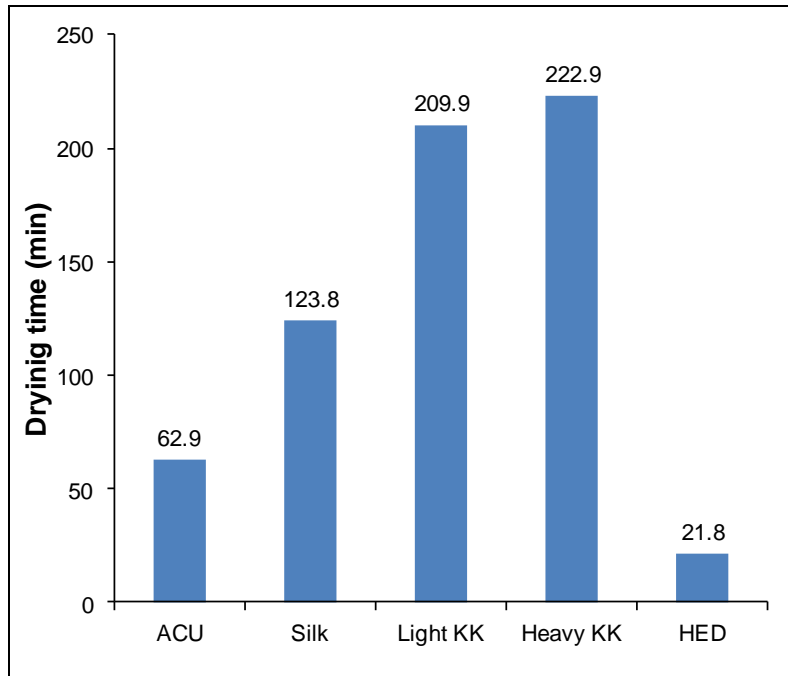


Figure 16. Drying time in minutes for different fabrics.

Table 9. Drying time in minutes for different fabrics.

Sample ID	Drying time (min)
ACU	62.9
Silk	123.8
Light KK	209.9
Heavy KK	222.9
HED	21.8

3.1.6 Horizontal Wicking

Figure 17 and table 10 show the horizontal wicking results. The ACU and knit samples show higher transport along the machine (warp) direction. The HED sample did not result in any wicking transport due to its strong water repellency.

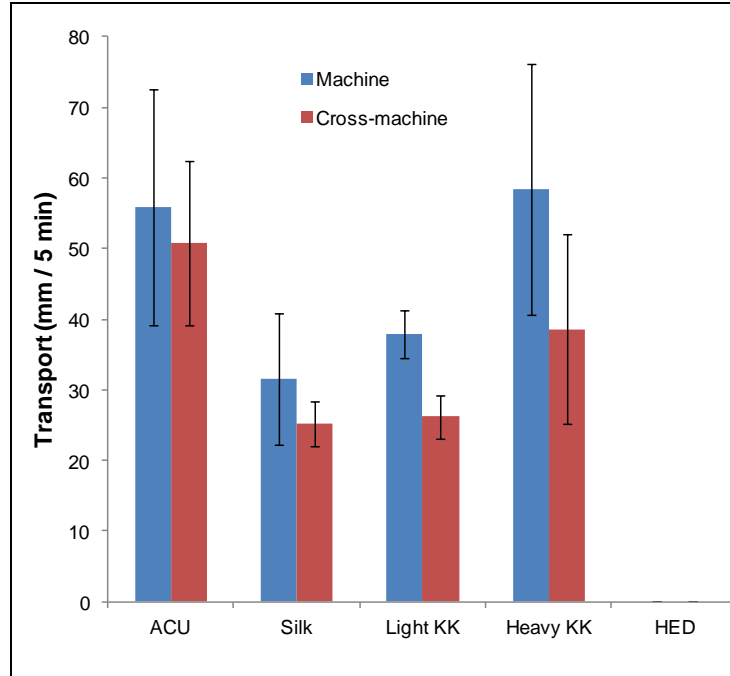


Figure 17. Horizontal liquid transport in millimeters per 5 min.

Table 10. Horizontal liquid transport in millimeters per 5 min.

	<u>ACU</u>		<u>Silk</u>		<u>Light KK</u>		<u>Heavy KK</u>		<u>HED</u>	
	Machine	Cross machine	Machine	Cross machine	Machine	Cross machine	Machine	Cross machine	Machine	Cross machine
	53.34	48.26	45.72	27.94	39.37	29.21	88.9	60.96	0	0
	40.64	40.64	20.32	22.86	35.56	27.94	53.34	35.56	0	0
	73.66	63.5	30.48	22.86	35.56	22.86	50.8	33.02	0	0
	none	none	33.02	29.21	43.18	27.94	43.18	25.4	0	0
	none	none	27.94	22.86	35.56	22.86	55.88	38.1	0	0
Average	55.88	50.8	31.496	25.146	37.846	26.162	58.42	38.608	0	0
Std Dev	16.66	11.64	9.26	3.16	3.41	3.06	17.69	13.37	0.00	0.00
Ranking	4	5	2	2	3	3	5	4	1	1

3.2 Mechanical Properties

3.2.1 Uniaxial Bending Stiffness

Figure 18 and table 11 show the uniaxial bending results. Silk shows nearly negligible bending rigidity, a reflection of its extremely high “drapability.” The ACU, light KK, and HED show similar rigidity, with heavy KK exhibiting the highest rigidity.

In bending stiffness and flexural rigidity evaluation, silk ranks the best; ACU, light KK, and HED rank second, followed by heavy KK third.

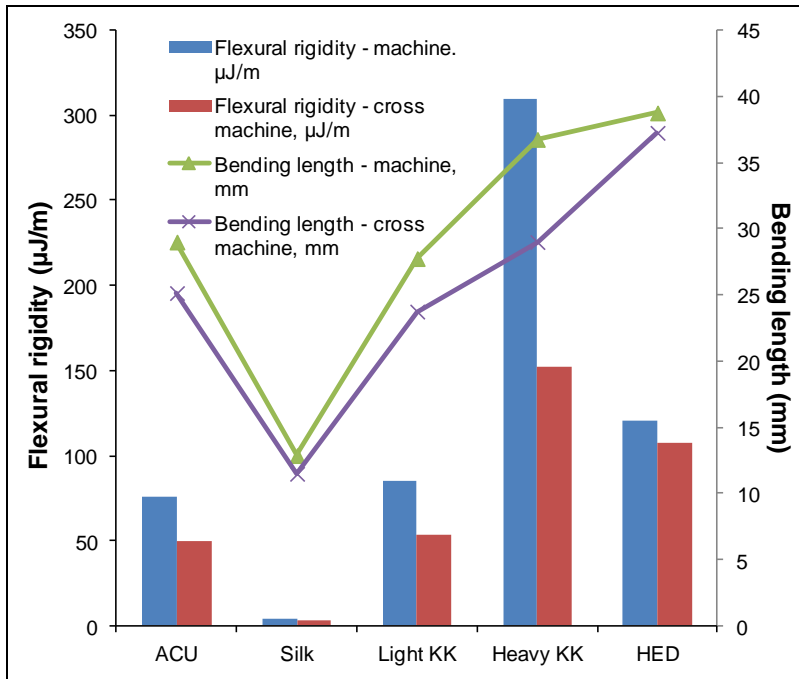


Figure 18. Uniaxial stiffness test results—bending stiffness and flexural rigidity.

Table 11. Bending stiffness and flexural rigidity from uniaxial bending tests.

Sample ID Direction		Bending length (mm)	Flexural rigidity (μJ/m)
ACU	warp	29.0	76.1
	fill	25.2	49.6
Silk	wales	12.9	4.46
	courses	11.5	3.18
Light KK	warp	27.8	85.0
	fill	23.8	53.3
Heavy KK	warp	36.8	309
	fill	29.0	152
HED	machine	37.3	107
	cross	38.8	121

3.2.2 Circular Bending Stiffness

Figure 19 gives load and displacement data for each tested fabric. A logarithmic scale was used in figure 19b to show load displacement data for fabrics whose data are not readily seen on the linear scale illustrated in figure 19a. These figures demonstrate the vast range of mechanical response seen among the collection of fabrics for this particular test. Peak loads for tested fabrics ranged from 0.19 N in silk to 43.3 N in ArmorFelt, and, in general, occurred after the plunger had translated 20–40 mm from its initial position. Felted materials (e.g., ArmorFelt and HED) exhibited the most resistance to bending through the aperture, followed by the woven K706 and KK fabrics. The baseline ACU and experimental CFKA materials exhibited load extension profiles similar to that seen of light KK. Low areal density knits (e.g., silk and polyester) exhibited the least resistance to bending, which is most readily seen in figure 19b. Figure 20 and table 12 show maximum loads generated during the circular bend test for each fabric. Note that the highest load material, ArmorFelt, is also the thickest material tested (see table 1), perhaps indicating that fabric thickness may influence test results due to the fixed gap (6.35 mm) between the plunger and orifice in the test apparatus. Thickness is not the only determinant, however, as the HED material, at 0.83 mm thick, showed considerably higher bending resistance than the thicker light KK (1.23 mm) and heavy KK (1.63 mm) materials.

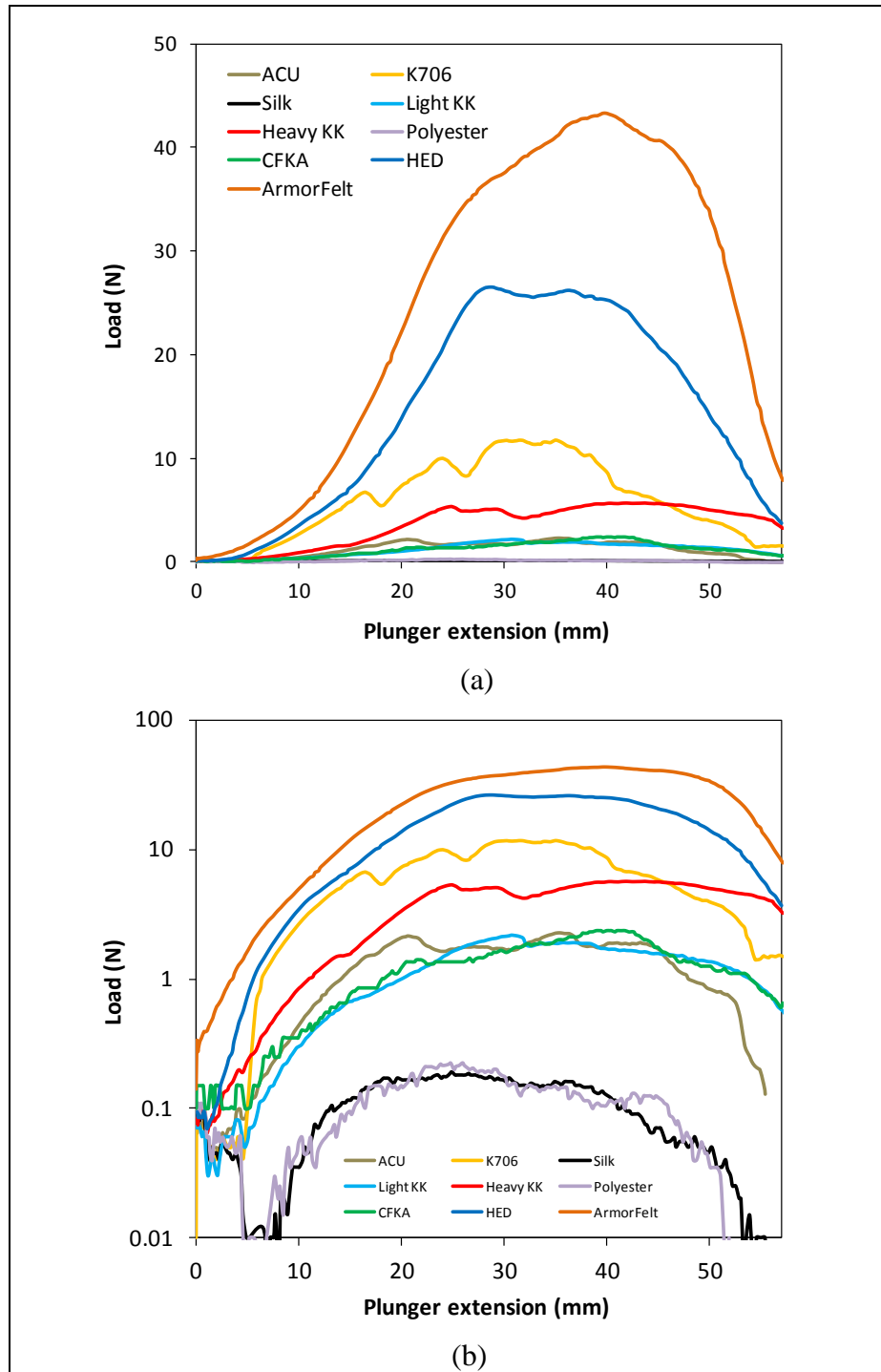


Figure 19. Load displacement data for circular bend test: (a) linear scale and (b) log scale.

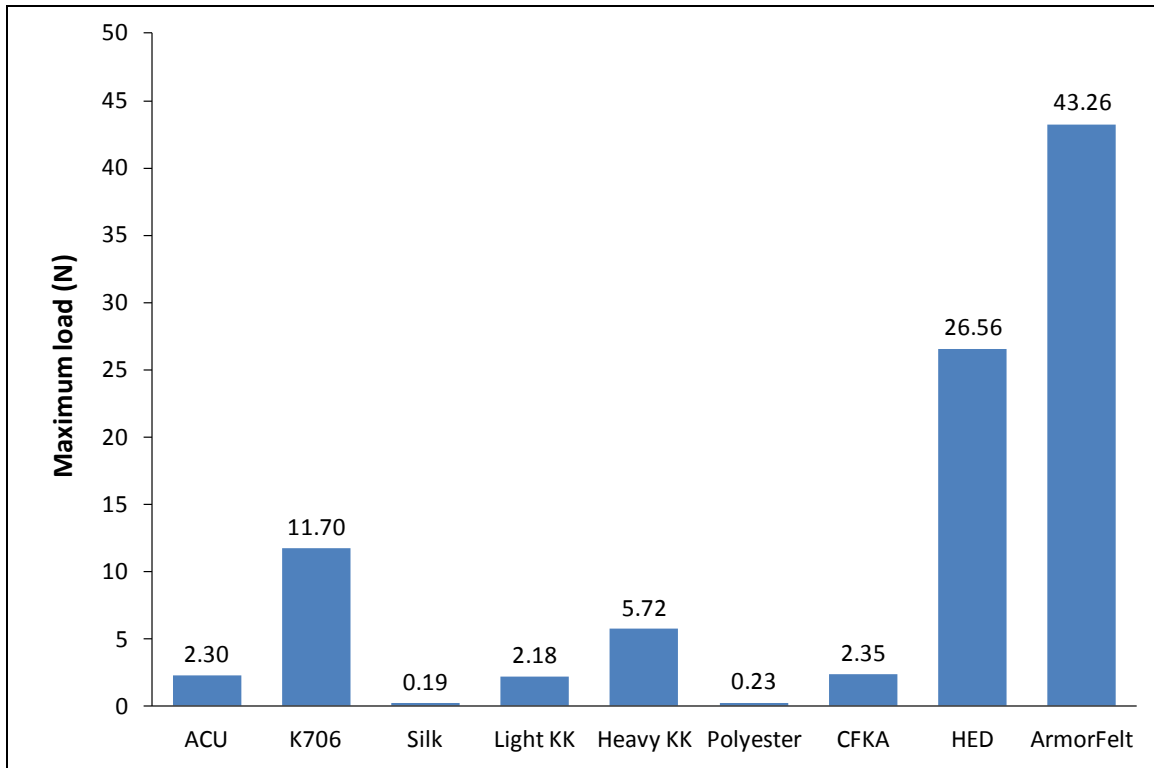


Figure 20. Maximum loads generated during circular bend test.

Table 12. Maximum loads during circular bend test.

Sample ID	Maximum load (N)
ACU	2.30
K706	11.70
Silk	0.19
Light KK	2.18
Heavy KK	5.72
Polyester	0.23
CFKA	2.35
HED	26.56
ArmorFelt	43.26

3.2.3 Stretchability

Figure 21 gives load displacement data for each tested fabric plotted on a logarithmic scale, as the mechanical response spans several decades of load. Table 13 summarizes the peak force values. Maximum crosshead displacement was limited to 8 mm due to the tendency of stiffer, woven fabrics to fail at the grips, which is evident in the load extension behavior of TexTech and K706 shown in figure 21. Both fabrics undergo rapid loading at the outset of the test and then strain with little change in load. Tearing at the grips was observed during the latter segment of the test. The woven-felt hybrid material TexTech provided the highest resistance to stretch, followed closely by the woven K706. Both fabrics exhibited maximum loads of over 1000 N. The low areal density knits were the most compliant fabrics, exhibiting maximum loads below 1 N at comparable displacement values. The light KK provided the least resistance to stretch. The baseline ACU, felts, and heavy KK provided intermediate responses, each exhibiting 1- to 20-N maximum loads.

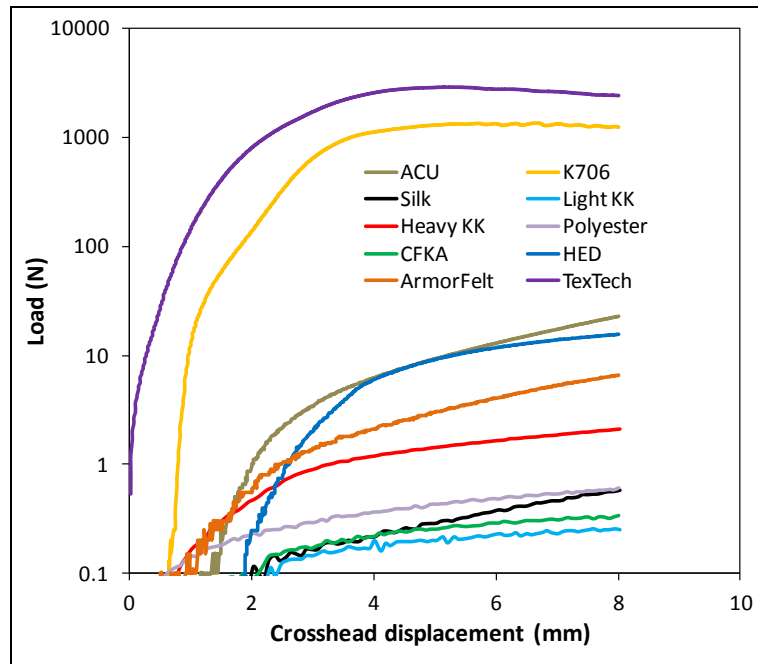


Figure 21. Load extension data for stretch test.

Table 13. Maximum loads during stretch test.

Sample ID	Maximum load (N)
ACU	22.55
K706	1338
Silk	0.58
Light KK	0.26
Heavy KK	2.09
Polyester	0.62
CFKA	0.34
HED	15.75
ArmorFelt	6.60
TexTech	2887

3.2.4 Knee-Bend Test

Figure 22 gives normalized load displacement data for each tested fabric subject to the knee-bend test. The felts and KK fabrics exhibited load displacement profiles characterized by a sharp increase in load at the outset of the test followed by a gradual increase in load until the completion of the test. ArmorFelt provided the greatest contribution to bending resistance in this configuration. The silk and CFKA provided the least resistance to bending; in fact, figure 22 indicates a negative contribution to bending resistance after normalization. This result is likely due to additional breaking-in of the foam cylinder as the tests occurred. The baseline ACU material performed similarly to polyester, with slightly higher resistance provided for the first 50 mm of crosshead displacement. Maximum normalized loads spanned from 0.575 N in silk to 12.7 N in ArmorFelt. Figure 23 shows the maximum normalized loads attained for each fabric and allows for an easy visual comparison.

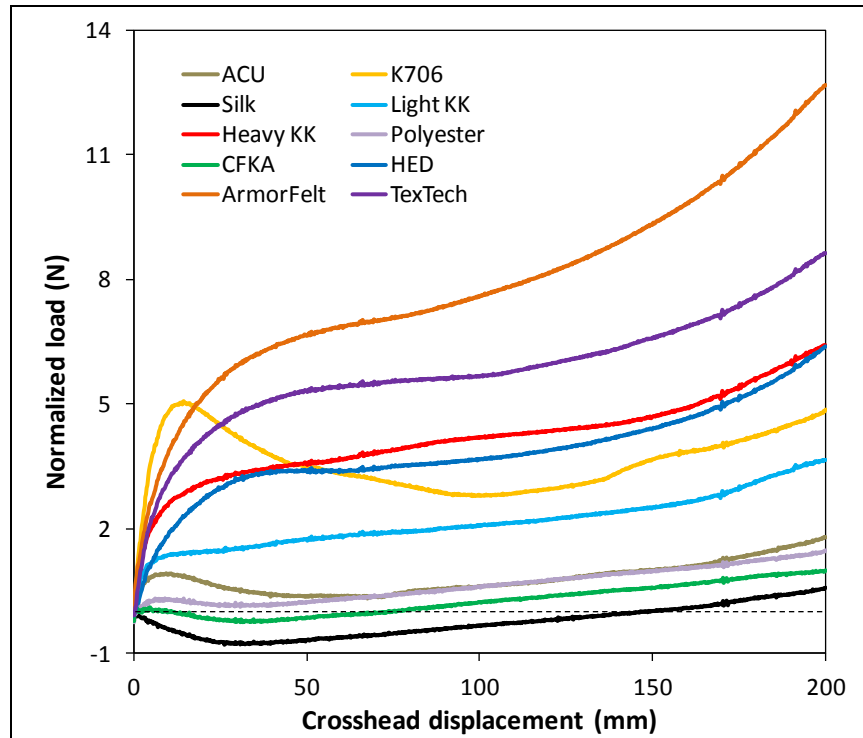


Figure 22. Normalized load displacement data for knee-bend test.

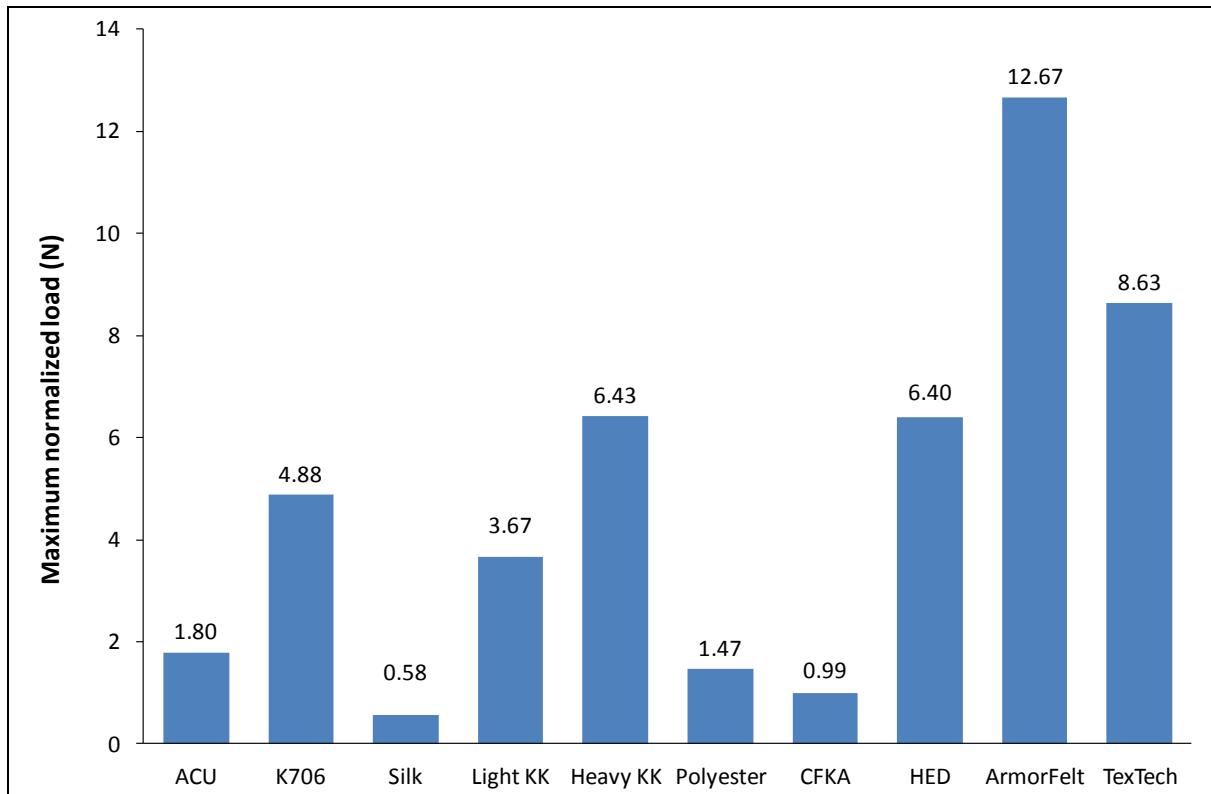


Figure 23. Maximum normalized load data during knee-bend test.

4. Discussion

4.1 Transport Properties

The water permeability experiments indicate that all materials evaluated provide reasonable levels of water through-thickness transport. For comparison, a prior study (16) found that thermoplastic-based woven and unidirectional fabrics (e.g., Argus and SpectraShield materials) subject to similar body-temperature experiments resulted in transport properties more than one order of magnitude lower ($<10 \text{ g/h m}^2$) than the samples evaluated in the present report. Of the materials tested, the more open structures (such as knit Kevlars) tended to result in higher moisture permeability than the more tightly woven fabrics such as ACU and K706.

The differences in air permeability were somewhat more pronounced, with the knits again providing higher transport than the ACU materials. It is interesting to note that the air permeability for the HED felt was also relatively low while its water vapor permeability was comparable to the knits. This result suggests that the tortuosity of the felt is more significant for the air permeability test than the moisture permeability test. This trend is logical, as the volumetric air flow during the air permeability test is significantly higher than the volumetric air flow during the water vapor permeability test.

The liquid moisture management results suggest that most of the knits will be rated “Very Good”; that is, they will effectively transport sweat away from the skin. It is surprising that the MMC rating for the heavy KK was significantly lower than for the light KK; more testing is required to determine if this trend is repeatable. The “Poor” MMC rating for the HED felt is likely due to the fact that it is very nonwetable. Similarly, the horizontal wicking capability of the HED is very low. Sweat will likely build up and pool on the skin, which limits further evaporative cooling. This effect should be considered if HED is integrated into near-skin garments.

The drying time data presents a somewhat contrasting trend. The HED felt exhibits the shortest drying trend, a result that is not surprising considering that water does not readily wet the fabric. So while HED likely will be uncomfortable with respect to sweating, if the HED felt were subject to water from, for example, rain, wading a body of water, or hand washing, it will likely dry quickly and be ready to wear sooner than the other fabrics.

4.2 Mechanical Properties

The uniaxial bending test shows that the silk fabric has the lowest rigidity. The results also indicate that the heavy KK knit gives the highest average rigidity—higher even than the HED felt. This result is very surprising, as, by hand feel, the HED feels significantly stiffer. The

circular bend test, in contrast, shows a more expected trend: the knits are most flexible; wovens have intermediate flexibility; and the felts have the lowest flexibility. Based on these trends, the circular bend test appears to give more reliable data than the uniaxial bend test.

One concern with the circular bend test is the dependence on sample thickness. Figure 24 plots peak load from circular bend testing as a function of fabric thickness. There is a general increasing trend in load with thickness. Although one would expect thickness to correlate with resistance to bending, the possibility remains that thickness unduly influences circular bend testing. Outliers include the K706 and HED fabrics, which appear to produce an unusually high bending resistance for their thickness. Figure 25 plots circular bend maximum loads normalized by fabric thickness. K706 and HED are shown as unusually stiff. Silk and polyester have the lowest per-thickness bending resistance. More research is required to determine what normalization strategy is most appropriate for circular bend data.

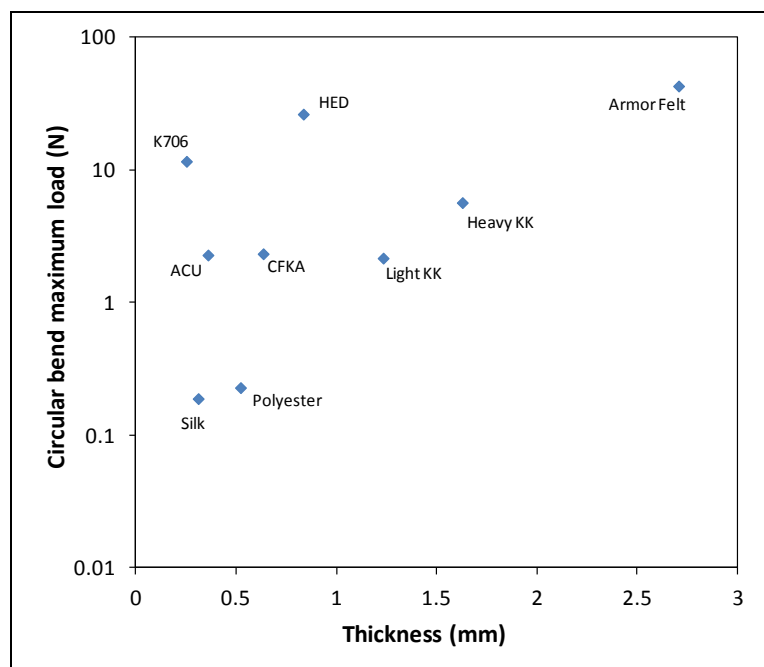


Figure 24. Circular bend peak load as a function of fabric thickness.

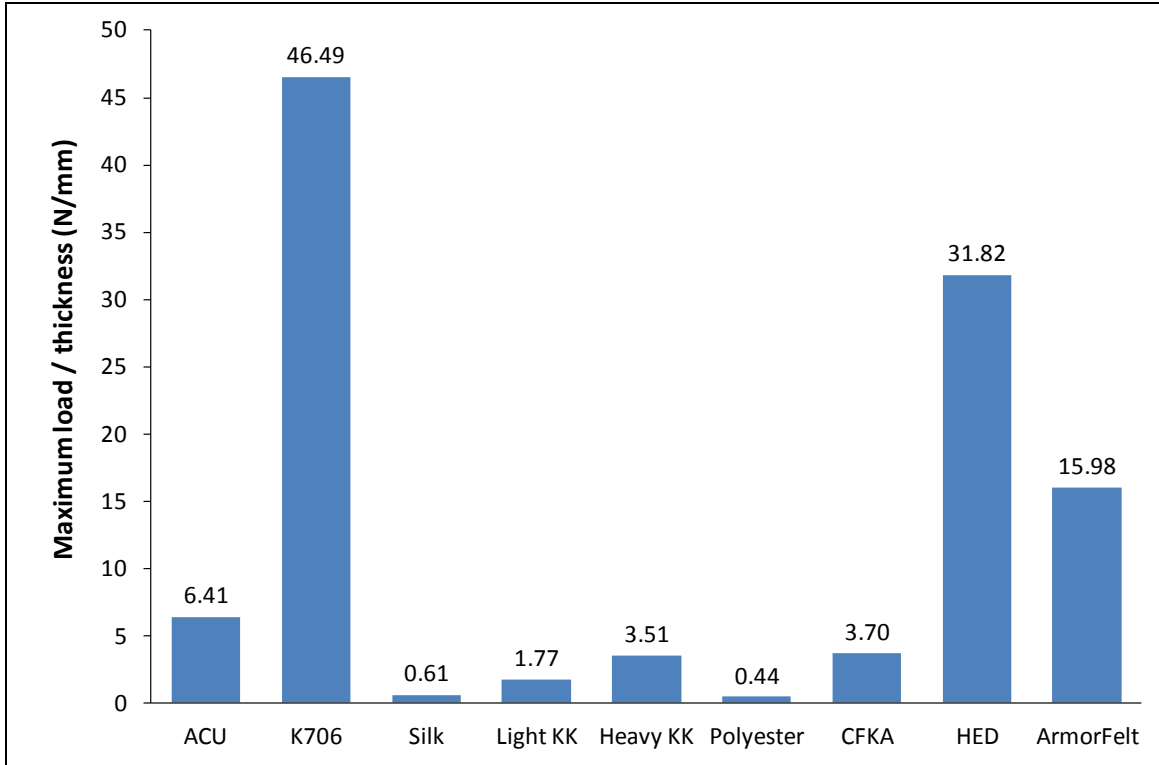


Figure 25. Thickness-normalized maximum load data from circular bend test.

The stretch test, not surprisingly, shows that the knits are the most stretchable. The pure felts (HED and ArmorFelt) show intermediate levels of stretch while the aramid wovens (K706 and TexTech, which has one layer of woven aramid) show very high resistance to stretch. This trend result is due to the fact that the woven aramids have low-crimp yarns, and the samples were stretched along the yarn direction. If the samples were, instead, oriented along the bias (45°) direction, more stretching would be noted.

The knee-bend test indicates that knits are most amenable to the knee-bending action while the felts are generally more resistive. The woven K706 provides intermediate response while, interestingly, the heavy KK again shows a relatively high resistance to motion. In general, these results seem to track more closely with the bending results than the stretch results, perhaps indicating that the knee test is mostly dominated by bending effects. Since the knee test is a novel and unproven apparatus, more testing is needed before strong conclusions can be made.

Note that no attempt was made to normalize the bending or stretching experiments with respect to areal density or thickness. For example, figure 26 shows the knee-bend peak force data (table 14) normalized by the areal density of each fabric (table 1). The light and heavy KK fabrics are now more comparable in performance, and the HED felt shows higher resistance than any of the wovens or knits. Interestingly, the TexTech fabric's relative resistance is significantly lower for the normalized data. More testing is required to confidently state what type of normalization is most appropriate for the mechanical test data.

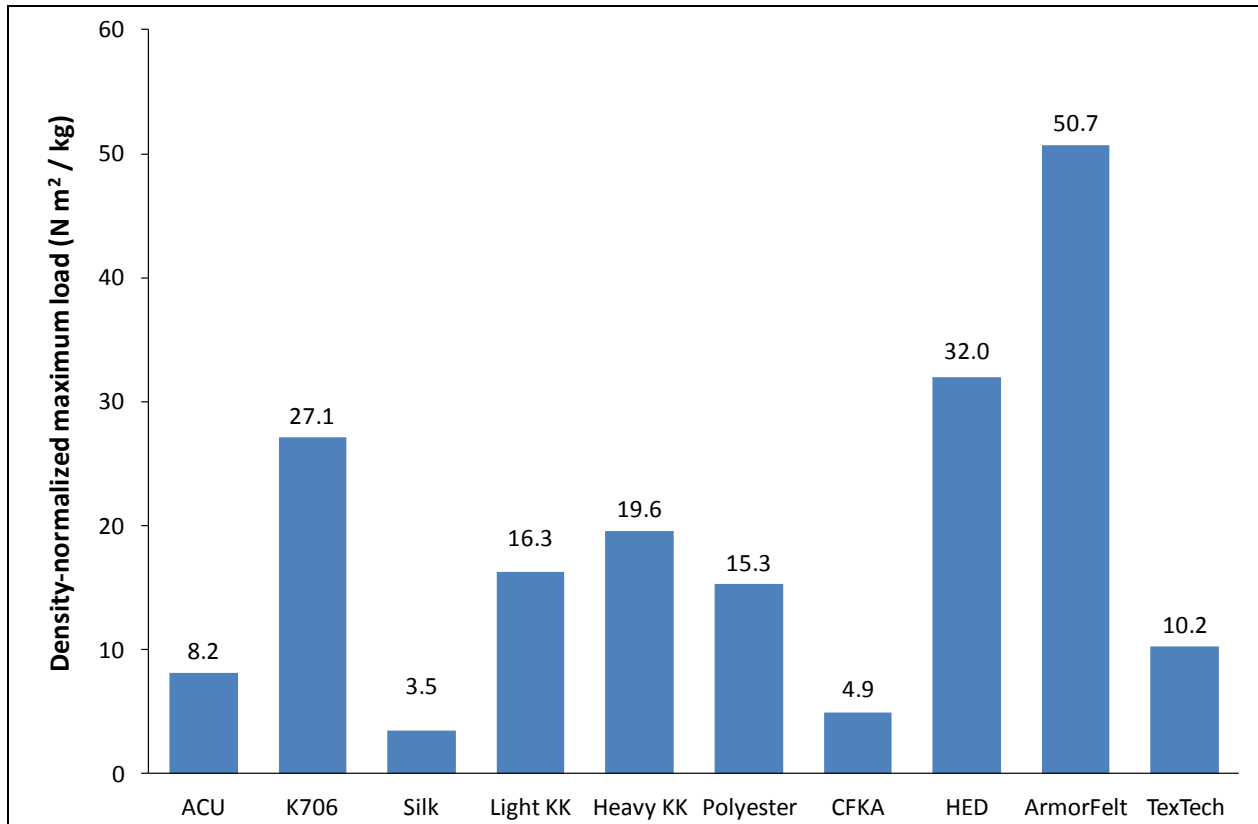


Figure 26. Density-normalized maximum load data from knee-bend test.

Table 14. Maximum normalized loads during knee-bend test.

Sample ID	Maximum normalized load (N)
ACU	1.80
K706	4.88
Silk	0.58
Light KK	3.67
Heavy KK	6.43
Polyester	1.47
CFKA	0.99
HED	6.40
ArmorFelt	12.67
TexTech	8.63

4.3 Implications for Comfort

The objective of this report was to collect material property data that provides guidance on the eventual comfort of garments composed of these fabrics. Some trends are evident, for example the knits in general appear to provide the best combination of low resistance to mechanical action with high air/vapor transport. The HED felt presents some concerns with respect to moisture management, and the felts in general also appear to be less suitable for applications requiring bending and stretch. These test results, however, are not sufficient to make subtle judgments about which knits will work best, or how much less comfortable the woven fabrics will feel relative to the knit fabrics. A more detailed set of experiments, with human subject trials, is required to begin such correlations. Note that any human subject trials likely will require manufacture of garments; the details of garment design and fit will further complicate the assessment of fabric comfort.

4.4 Correlating Comfort With Ballistic Performance

For armor design, fabric comfort values must also be evaluated relative to ballistic performance. That is, very comfortable materials that do not provide protection are not inherently useful as armor, while materials that offer good ballistic protection but are very uncomfortable are not likely to be accepted as fielded items. Determining the appropriate balance of ballistic and comfort properties is a significant challenge.

As an example of how one might begin to assess the data, table 15 calculates areal-density-normalized ballistic performance data, based on results from Michael et al. (5), for gel-backed glass-sphere ballistic testing. Also shown in the table is the knee-bend test data, as normalized by the specimen areal density (the knee-bend experiments were all performed on single-layer samples). Figure 27 plots the ballistic metric as a function of the comfort metric. Better-performing materials should tend toward the upper left of the plot. Materials like ArmorFelt appear to have good ballistic properties but poor comfort. ACU fabric, in contrast, has good comfort but poor ballistics. The CFKA material appears to provide a relatively good balance of comfort and ballistic performance.

The comparison in figure 27 is provided only as an example of how such assessments could be made. Many more ballistic and comfort metrics could be valid, and the precise balance of these metrics that are optimal will be application and garment specific. More research is required to improve our ability to make effective design decisions based on such metrics.

Table 15. V_{50} and knee-bend test data normalization. Ballistic data from Michael et al. (5).

Sample ID	Number of layers	Target AD (g/m ²)	V_{50} (m/s)	V_{50} / AD (m ³ /s/g)	Density-normalized max knee bend load (N m ² /kg)
ACU	2	440	205	0.466	8.16
K706	2	360	290	0.807	27.12
Silk	2	330	194	0.588	3.48
Light KK	2	450	213	0.474	16.31
Heavy KK	1	328	191	0.581	19.59
Polyester	4	384	196	0.511	15.29
CFKA	2	400	271	0.677	4.94
HED	2	400	367	0.917	31.99
ArmorFelt	2	500	387	0.774	50.66
TexTech	1	844	413	0.489	10.22

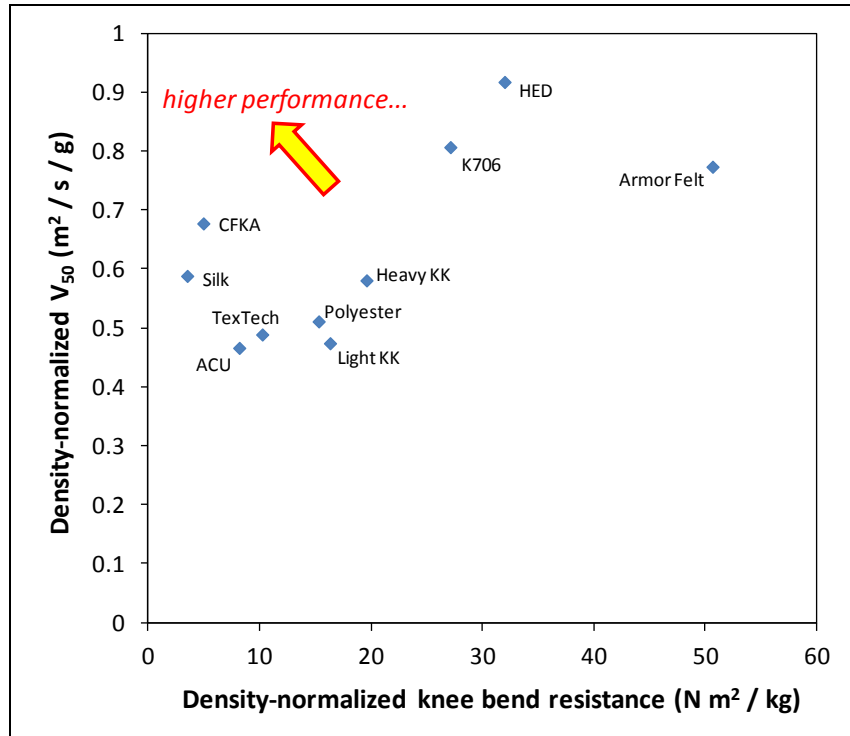


Figure 27. Ballistic metric (density-normalized V_{50}) as a function of comfort metric (density-normalized knee-bend force).

5. Conclusions

This study documents a wide range of textile material properties relevant to garment comfort, including air and vapor transport properties and mechanical properties. The tests undertaken in this study are not comprehensive. Additional comfort-relevant characterizations include guarded sweating hotplate test (17), Kawabata tests (18), and the Cusick drape test (19).

In general, knits appear to provide the best combination of breathability and ease of deformation, and should be amenable to incorporation into comfortable garments. Woven textiles are less breathable and very difficult to stretch along their principal yarn directions, but could still be useful in on areas of the garment that are not required to stretch. Felts offer low air permeability but permit acceptable levels of moisture vapor transport, tend to be thick, are somewhat stretchable, but are also resistant to bending. The felt composed of ultrahigh molecular weight polyethylene, in particular, is highly nonwetting to liquid water and therefore may be uncomfortable to wear close to the skin while sweating.

These insights, while useful, are not sufficiently comprehensive to enable selection and design of garments with optimal comfort. Subtle differences in performance cannot be determined from these material tests, and some test results imply conflicting conclusions. Garment fabrication and human subject testing are still required to provide a more complete understanding of function and comfort.

Furthermore, for personnel protection, comfort performance must be balanced against ballistic performance. The quantitative tools necessary for systematically comparing materials across an array of performance requirements do not yet exist. More research is necessary to develop these design tools. Numerical simulations of textile systems already exist (20), and the application of these models to comfort predictions are in their early stages (21). Developing these models, coupled with ballistic and casualty models, could lead to a holistic, predictive simulation environment for design and optimization of protective garments.

6. References

1. North Carolina State University, College of Textiles, Textile Protection and Comfort Center Home Page. <http://www.tx.ncsu.edu/tpacc/comfort-performance/> (accessed 11 February 2013).
2. Janski, L.; Ulbricht, V. Textile Drape as Mechanical Phenomenon. *Proceedings in Applied Mathematics and Mechanics* **2002**, *1* (1), 223–224.
3. ASTM F 1868-12. Standard Test Method for Thermal and Evaporative Resistance of Clothing Material Using a Sweating Hot Plate. *Annu. Book ASTM Stand.* **2012**.
4. Horsfall, I.; Champion, S. M.; Watson, C. H. The Development of a Quantitative Flexibility Test for Body Armour and Comparison With Wearer Trials. *Appl. Ergon* **2005**, *36* (3), 283–292.
5. Michael, W.; Dalzell, L. R.; Long, K. A.; Slusarski, S. A.; Fossey, P. J.; Wetzel, E. D. *Ballistic Characterization of Fabrics for Groin and Extremity Protection, Including Continuous-Filament Knit Aramids*; ARL-TR-6412; U.S. Army Research Laboratory: Aberdeen Proving Ground, MD, April 2013.
6. Pincus, W. Military Bulks Up to Protect Against Groin Injuries. *The Washington Post* [online], 18 August 2011. http://www.washingtonpost.com/blogs/checkpoint-washington/post/military-bulks-up-to-protect-against-groin-injuries/2011/08/18/gIQAq6ZPOJ_blog.html (accessed 19 August 2011).
7. MOD Introduces Pelvic Protection for Frontline Troops. *Defence News* [online], 17 December 2010. <http://www.mod.uk/DefenceInternet/DefenceNews/EquipmentAndLogistics/ModIntroducesPelvicProtectionForFrontLineTroops.htm> (accessed 16 November 2012).
8. ASTM D 1777-96. Standard Test Method for Thickness of Textile Materials. *Annu. Book ASTM Stand.* **2011**.
9. ASTM E 96/E 96M-10. Standard Test Methods for Water Vapor Transmission of Materials. *Annu. Book ASTM Stand.* **2010**.
10. AATCC Test Method 195-2011. Liquid Moisture Management Properties of Textile Fabrics. American Association of Textile Chemists and Colorists, Research Triangle Park, NC, 2011.
11. ASTM D 737-04. Standard Test Methods for Air Permeability of Textile Fabrics. *Annu. Book ASTM Stand.* **2008**.
12. Drying Time Test Method. U.S. Army Natick Soldier Research, Development, and Engineering Center, Natick, MA, 2010.

13. AATCC Test Method 198-2011. Horizontal Wicking of Textiles; American Association of Textile Chemists and Colorists, Research Triangle Park, NC, 2012.
14. ASTM D 1388-08. Standard Test method for Stiffness of Fabrics. *Annu. Book ASTM Stand.* **2008**.
15. ASTM D 4032-08. Standard Test Method for Stiffness of Fabric by the Circular Bend Procedure. *Annu. Book ASTM Stand.* **2008**.
16. Chin, W. K.; Wetzel, E. D. *Breathability Characterization of Ballistic Fabrics, Including Shear Thickening Fluid-Treated Fabrics*; ARL-TR-4392; U.S. Army Research Laboratory: Aberdeen Proving Ground, MD, March 2008.
17. Huang, J. Sweating Guarded Hot Plate Test Method. *Polymer Testing* **2006**, 25 (5), 709–716.
18. Kawabata, S.; Niwa, N. Objective Measurement of Fabric Mechanical Property and Quality: Its Application to Textile and Clothing Manufacturing. *Int. J. Clothing Sci. and Tech.* **1991**, 3 (1), 7–18.
19. Hu, J.; Chan, Y.-F. Effect of Fabric Mechanical Properties on Drape. *Textile Research Journal* **1998**, 68 (1), 57–64.
20. Nilakantan, G.; Keefe, M.; Bogetti, T. A.; Gillespie, J. W., Jr. Multiscale Modeling of the Impact of Textile Fabrics Based on Hybrid Element Analysis. *International Journal of Impact Engineering* **2010**, 37 (10), 1056–1071.
21. Keefe, M.; Wetzel, E. D. Modeling and Simulation of Fabric-Human Interactions. *Proceedings of TexComp-11 Conference*, Leuven, Belgium, 16–20 September 2013; in press.

NO. OF
COPIES ORGANIZATION

1 DEFENSE TECHNICAL
(PDF) INFORMATION CTR
DTIC OCA

1 DIRECTOR
(PDF) US ARMY RESEARCH LAB
IMAL HRA

1 DIRECTOR
(PDF) US ARMY RESEARCH LAB
RDRL CIO LL

1 GOVT PRINTG OFC
(PDF) A MALHOTRA

5 RDRL WMM A
(3 HC, W CHIN (3 HC, 1 PDF)
2 PDF) E WETZEL

8 US ARMY NATICK SOLDIER
(HC) RD&E CTR
E WELSH
C/O S FOSSEY
R-311
15 KANSAS ST
NATICK MA 01760-5020

2 US ARMY NATICK SOLDIER
(HC) RD&E CTR
TMET
S GASSETT
15 KANSAS ST
NATICK MA 01760-5020

4 PRODUCT MGR SOLDIER
(HC) PROTECTIVE EQUIPMENT
R ROZANSKY
10170 BEACH RD
BLDG 328T
FORT BELVOIR VA 22060

INTENTIONALLY LEFT BLANK.